# Thin Film Orientation by Epitaxy of Carbazolyl Polydiacetylenes: Guest−Host Interaction on a Crystal Surface

**V. Da Costa,[†] J. Le Moigne,*[,†] L. Oswald,[†] T. A. Pham,[†] and A. Thierry[‡]**

*Institut de Physique et Chimie des Matériaux de Strasbourg, UMR 7504, 23 rue du Loess BP 20, 67037 Strasbourg, and Institut C. Sadron, 6 rue Boussingault, 67083 Strasbourg, Cedex, France*

*Received August 4, 1997; Revised Manuscript Received December 22, 1997*

ABSTRACT: We investigated the oriented overgrowth of a series of diacetylene molecules by *epitaxy* on a single crystal of potassium acid phthalate (KAP). By changing the chemical architecture of the deposited molecule, we were able to modify the molecular interactions between the deposited molecule and the crystal surface. Thus we synthesized four new asymmetrical diacetylenes (DA) bearing a carbazolyl group on one side of the diacetylene core and a urethane at the end of a flexible spacer on the other side of the DA moiety. The different conditions of the film growth under high vacuum were implemented by a systematic investigation of the different kinetic parameters acting on the molecule arrangement at the crystal surface, such as the monomer evaporation rate or the substrate temperature. The morphology and the structure of the films were studied by atomic force microscopy (AFM) imaging and transmission electron microscopy (TEM) and compared to the morphologies of the bis(carbazolyl) derivative {poly[1,6-bis(9-carbazolyl)-2,4-hexadiyne], abbreviated pDCH}. We found, for the *monosubstituted carbazolyl derivative* {poly[9-(9-carbazolyl)-5,7-nonadiyn-1−ol ethylurethane], abbreviated (pCNEU)}, that the molecular interactions leading to epitaxy were of several types on the (010) plane of KAP. First, a $\pi-\pi$ type interaction induced one prevailing *position* of the DA molecules (the aromatic sides of the carbazolyl substituent were inserted between phenyl rows of KAP stacked along *c*). Second, another geometrical interaction induced two secondary positions of the DA molecules (the flexible moiety lying in shallow ditches lined along the ⟨101⟩ directions of KAP). Related to the thin film morphologies, the static optical spectroscopies were also investigated and discussed. Improvements in orientational order were observed on pCNEU as on pDCH at slow evaporation rates and on heating the crystal substrate in the temperature range 50−100 °C.

## Introduction

The most commonly used techniques for the elaboration of oriented organic films on a substrate are the uniaxial shear techniques such as buffing,[1] rubbing, or the friction transfer.[2] Orientation occurs also in thin single crystals[3] or as overgrowth on single crystals.[4,5] As far as polymers are concerned, the orientation can be induced before or after polymerization by uniaxial shear techniques. Some of the polymers can be oriented by organic molecular beam epitaxy (OMBE), whereby the monomer is oriented prior to the solid state polymerization. For nonlinear optical applications the molecular beam epitaxy technique often gives rise to better quality, highly transparent thin films. Thin films for second- or third-order nonlinear applications are well oriented by epitaxial growth on single crystals[6,7] or on preoriented thin films.[8] Depending on their molecular symmetry, they show a strong linear dichroism, as observed by UV−vis spectroscopic measurements, and also a strong nonlinear anisotropy, which are very interesting for nonlinear investigations.[9,10] Polydiacetylene (PDA) is one of the most interesting classes of polymers and has attracted a great deal of attention due to the very important delocalization of the $\pi$ electrons along the conjugated chains.[11] PDAs are crystalline polymers obtained by solid-state polymerization of the monomer crystals (DA). But even though single crystals have been investigated, defect-free single crystals of PDA are usually difficult to grow,[12] especially for large thin single crystals.[3] To obtain uniaxially well oriented thin films for nonlinear optics, a few years ago we investigated the epitaxial growth of a variety of hyperpolarizable molecules.[9,13] For third-order nonlinear optics we used a symmetrically substituted diacetylene monomer [1,6-bis(9-carbazolyl)-2,4-hexadiyne (abbreviated DCH)] that was evaporated under high vacuum on a single crystal of potassium acid phthalate (KAP), resulting in highly oriented samples. The single orientation of the monomer crystals in the film is conserved during the thermal polymerization. The good orientation of the poly[1,6-bis(9-carbazolyl)-2,4-hexadiyne] chains (abbreviated pDCH) has been confirmed by the high dichroic ratio of the optical spectra measured with polarized incident light.[14] It can be inferred that the molecular epitaxy between the DCH monomer and KAP was due to geometrical interaction between the two carbazolyl groups and phenyl rows of KAP.

To ascertain the molecular interaction of the substituted diacetylenes with the substrate, we synthesized four new asymmetrical monomers with only a single carbazolyl group. The second substituent of the diacetylene consists of a urethane group ended by a phenyl or an alkyl moiety. Thus by changing the end group and the topology of the molecule we are able to modify the local interactions between the guest molecule and the phenyl rings of the host crystal surface. Due to the spacer effect between the diacetylene core and the urethane block, the configuration of the end group (i.e. the position of the urethane H bond of the side chains) is strongly different for molecules with an odd and an even number of carbons. Another reason for the choice of the urethane group was the necessity to obtain highly polymerizable diacetylenes in the solid state.[15]

[†] Institut de Physique et Chimie des Materiaux de Strasbourg.
[‡] Institut C. Sadron.

S0024-9297(97)01177-7 CCC: $15.00 
Published on Web 02/19/1998

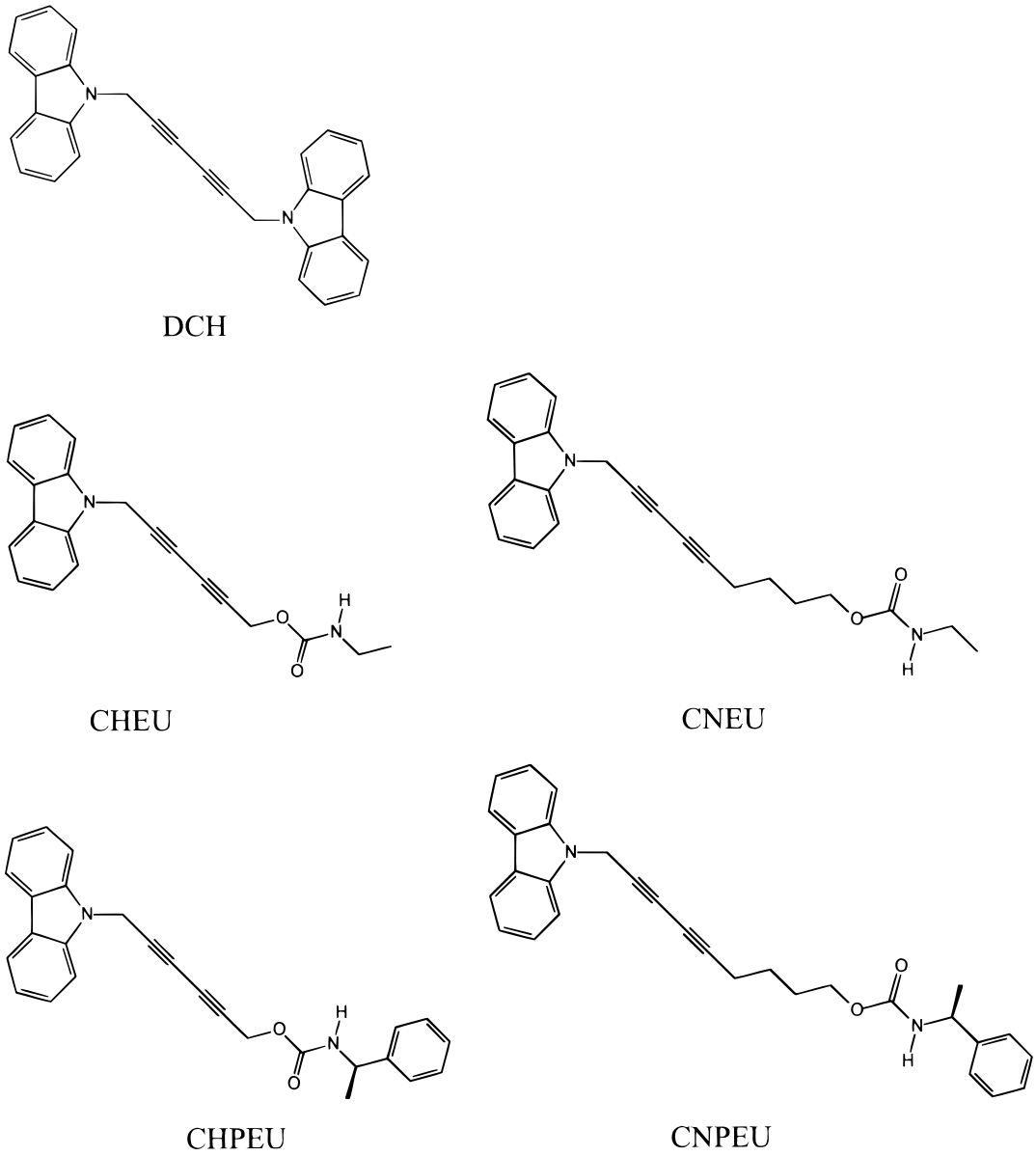


**Figure 1.** DCH and the asymmetrical diacetylenes of the DCH family synthesized in this work. The DA monomers are based on phenyl- or ethylurethane derivatives of 6-(9-carbazolyl)-2,4-hexadiyn-1-ol and 9-(9-carbazolyl)-5,7-nonadiyn-1-ol.

The diacetylene molecules bearing urethane side groups are good candidates.[16]

In the present work the oriented overgrowth on a KAP crystal of a single-carbazolyl diacetylene is studied with a systematic modification of the kinetic parameters (the substrate temperature and the deposition rate). The morphology and the orientation of the monomer and polymer films of both dicarbazolyl and single-carbazolyl DA are investigated by atomic force microscopy (AFM) imaging and by electron microscopy (TEM). In an attempt to relate the macroscopic optical properties to microscopic organization, we discuss also the optical spectroscopy and the observed film structure and morphology. The first part of our investigation is devoted to completing by AFM imaging our previous characterization[13] of the DCH monomer and polymer films. These results will be used as a reference for the second part, which is devoted to the analysis of the overgrowth of the asymmetrical carbazolyl DA series on the (010) plane of KAP. We conclude that the observed organizations of the thin films rely on the molecular interaction of the side groups.

## Experimental Section

We synthesized the two basic intermediates, the 6-(9-carbazolyl)-2,4-hexadiyn-1-ol **(1)** and 9-(9-carbazolyl)-5,7-nonadiyn-1-ol **(2)**, by asymmetrical coupling. The diacetylene coupling was followed by reaction of the OH group with the ethyl and the phenyl isocyanate derivatives to afford the urethane DA derivatives of Figure 1. Some of the asymmetrical diacetylenes bearing a single carbazolyl and different urethane groups have been synthesized according to the literature.[16,17] The other derivatives have been synthesized using the following route.

**6-(9-Carbazolyl)-2,4-hexadiyn-1-ol (1) and 9-(9-carbazolyl)-5,7-nonadiyn-1-ol (2)** were synthesized according to the paper of Yee.[16] **1**: white crystals; yield 71%; mp, 119−120 °C; $^1$H NMR (acetone-$d_6$) $\delta$ 8.15 (d, 2H, Ph H), 7.60 (d, 2H, Ph H), 7.47 (m, 2H, PhH), 7.25 (m, 2H, PhH), 5.41 (s, 2H, $-NCH_2-$), 4.32 (s, 1H, $-OH$), 4.18 (s, 2H, $-CH_2-$). Anal. Calcd for $C_{18}H_{13}NO$: C, 83.37; H, 5.05; N, 5.40. Found: C, 83.02; H, 4.99; N, 5.10. **2**: white crystals; yield 45%; mp, 105−107 °C; $^1$H NMR (acetone-$d_6$), $\delta$ 8.14 (d, 2H, Ph H), 7.64 (d, 2H, Ph H), 7.48 (m, 2H, PhH), 7.24 (m, 2H, PhH), 5.37 (s, 2H, $-NCH_2-$), 3.47 (m, 3H, $-CH_2O-$, $-OH$), 2.25 (t, 2H, $\equiv C-CH_2\,C-\,CH_2-$), 1.50 (m, 4H, $-CH_2-$). Anal. Calcd for $C_{21}H_{19}$-

NO: C, 83.69; H, 6.35; N, 4.65. Found: C, 83.91; H, 6.53; N, 4.56.

**9-(9-Carbazolyl)-5,7-nonadiyn-1−ol Ethylurethane (CNEU).** A solution of 2.1 g (0.030 mol) of ethyl isocyanate in 10 mL of 1,2-dimethoxyethane was added dropwise to a solution of **2** (7.2 g, 0.024 mol), 20 mL of 1,2-dimethoxyethane, 0.2 g of dibutyltin dilaurate, and 2 mL of triethylamine with vigorous stirring. After stirring at 40 °C for 2 h, 150 mL of heptane was added to the reaction mixture. The precipitate was collected by filtration, washed in heptane, and dried, resulting in 6.7 g of CNEU. Yield: 75%. Mp: 124−125 °C. $^1$H NMR ($CD_2Cl_2$): $\delta$ 8.10 (d, 2H, Ph H), 7.50 (m, 4H, Ph H), 7.28 (m, 2H, PhH), 5.12 (s, 2H, $-NCH_2-$), 4.63 (s, 1H, −NH−), 3.95 (t, 2H, $-CH_2O-$), 3.10 (m, 2H, $-CH_2CH_3$), 2.25 (t, 2H, $\equiv C-CH_2-$), 1.55 (m, 4H, $-CH_2-$), 1.07 (t, 3H, $-CH_3$). Anal. Calcd for $C_{24}H_{24}N_2O_2$: C, 77.39; H, 6.50; N, 7.52. Found: C, 77.16; H, 6.54; N, 7.40.

The same method was used then for the following DA.

**9-(9-Carbazolyl)-5,7-nonadiyn-1−ol−(1-Phenylethyl)-urethane] (CNPEU).** Yield: 89%. Mp: 123−124 °C. $^1$H NMR ($CDCl_3$): $\delta$ 8.10 (d, 2H, Ph H), 7.50 (m, 4H, Ph H), 7.27 (m, 7H, PhH), 5.11 (s, 2H, $-NCH_2-$), 4.87 (m, 2H, −NH−, −CH−), 4.02 (m, 2H, $-CH_2O-$), 2.23 (m, 2H, $\equiv C-CH_2-$), 1.60 (m, 4H, $-CH_2-$), 1.46 (d, 3H, $-CH_3$). Anal. Calcd for $C_{30}H_{28}N_2O_2$: C, 80.33, H, 6.29; N, 6.25. Found: C, 79.96; H, 6.33; N, 6.19.

**6-(9-Carbazolyl)-2,4-hexadiyn-1-ol−1-Ethylurethane (CHEU).** Yield: 69%. Mp: 127−130 °C. $^1$H NMR ($CD_2Cl_2$): $\delta$ 8.10 (d, 2H, Ph H), 7.50 (m, 4H, Ph H), 7.27 (m, 2H, PhH), 5.15 (s, 2H, $-NCH_2-$), 4.63 (s, 2H, $-CH_2O-$), 3.14 (m, 2H, $-CH_2CH_3$), 1.07 (t, 3H, $-CH_3$). Anal. Calcd for $C_{21}H_{18}N_2O_2$: C, 76.34; H, 5.49; N, 8.48. Found: C, 76.10; H, 5.46; N, 8.23.

**6-(9-Carbazolyl)-2,4-hexadiyn-1-ol−(1-phenylethyl)-urethane] (CHPEU).** Yield: 62%. Mp: 178−180 °C. $^1$H NMR ($CDCl_3$): $\delta$ 8.10 (d, 2H, Ph H), 7.49 (m, 4H, Ph H), 7.30 (m, 7H, PhH), 5.13 (s, 2H, $-NCH_2-$), 4.98 (s, 1H, −NH−), 4.74 (m, 3H, −CH−, $-CH_2O-$), 1.46 (d, 3H, $-CH_3$). Anal. Calcd for $C_{27}H_{22}N_2O_2$: C, 79.78; H, 5.46; N, 6.89. Found: C, 80.34; H, 5.45; N, 6.87.

The crystalline monomers are very sensitive to UV light and polymerize well to give red or pink crystals.

In previous works we have reported the preparation of oriented films of 1,6-bis (9-carbazolyl)-2,4-hexadiyne by epitaxial growth on alkali halide[18] and on potassium acid phthalate single crystals.[13] The experimental procedure developed during the film elaboration consists of the control of the growth kinetics of the diacetylene monomer films and then, in a further step, in the control of the solid-state polymerization parameters. During the first step of the procedure, we modified the evaporation rate and the substrate temperature, to act on the growth parameters and thus on the film morphology. In the second step of the procedure, the solid-state polymerization, temperature, and time of reaction were investigated.

The KAP single crystals were cleaved and then immediately introduced into the vacuum system. The crystal substrates, heated or cooled under vacuum, were maintained at constant temperature from −196 to +100 °C within ±2 deg. The film thickness was monitored in situ with a quartz microbalance. The evaporation rates of monomers were in the range 0.1−0.2 nm/min or 0.1−0.5 nm/s. During this evaporation, the residual pressure in the vacuum system was kept at $\sim 5 \times 10^{-8}$ mbar and $\sim 1 \times 10^{-7}$ mbar, respectively, for low and high evaporation rates. The polymerization of DCH on KAP was realized in situ under vacuum or ex situ in an oven at various temperatures. Optimized conditions are 150 °C during 24 h under an Ar or $N_2$ atmosphere.[19] The CNEU monomer was deposited under vacuum at different substrate temperatures from room temperature up to 100 °C. For CNEU the photopolymerization by irradiation at 254 nm occurs only after thermal treatment at 100 °C. For CHPEU the polymerization occurs after thermal treatment at 120 °C. CHEU was polymerized under the same conditions as CNEU, while CNPEU did not polymerize under these conditions. At each step of the film elaboration, the morphologies were characterized by AFM or TEM.

The AFM measurements were carried out with a Nanoscope III from Digital Instruments. The images were recorded using two operating modes: the tapping mode and the contact mode, respectively, for large scale and nanoscale resolution. The contact mode was performed for molecular resolution, for repulsive forces in the range of $10^{-8}$ N. The tapping mode, which is a noncontact mode technique, operates for forces in the range 0.1−1 nN. The force applied in tapping mode is significantly lower than the force applied by the contact mode.[20] The tapping mode is better for imaging the monomeric films because the adhesion forces of the monomer crystals with the substrate are low. In contact mode, we used a 12 $\mu$m scanner and standard cantilevers of 100 $\mu$m length with integrated $Si_3N_4$ tips and their force constant was 0.58 N/m. In the tapping mode we used 122 $\mu$m long cantilevers, which have a force constant close to 50 N/m. The resonant frequencies were in the range 200−400 kHz. The sharpest tips were selected in order to obtain the best resolution, and they have an estimated nominal radius close to 10 nm. The microscope operated at ambient atmosphere and room temperature.

The ultraviolet and visible absorption spectra were measured with a Hitachi U3000 UV−visible scanning spectrophotometer. TEM observations were performed on a Phillips CM12 microscope operated at 120 kV. The PDA films were shadowed by Pt/carbon deposition and reinforced by a second evaporated carbon film. The samples were floated on distilled water where the KAP substrate was solubilized. Then the resulting thin film was transferred to a microgrid. The preparation was observed at room temperature, thus preventing the observation of the monomer that instantaneously polymerizes under the electron beam in these experimental conditions.

The molecular modeling was performed using the software Sybyl from Tripos, running on an Indigo 2 work station from Silicon Graphics; statistical analysis of AFM pictures was performed using Khoros Software.

## Results and Discussion

The orientation of DA monomers occurs by epitaxy on a KAP single crystal for different evaporation conditions, i.e., at low and high evaporation rates and at various substrate temperatures. Very thin films, equivalent to a few monolayers were elaborated for AFM and TEM investigations of the nucleation and orientation of the growing crystal**s**. The electron diffraction patterns are analogous to those already published,[13] although they indicate a smaller angular dispersion of the chain axis, sign of an improvement in the single orientation. Thicker films of several tens of nanometers were prepared for the optical characterizations.

First, we investigated the surface of the KAP substrate by AFM. Figure 2a shows a crystal step in the (010) cleavage plane. The step is 1.34 nm high, which is close to the cell parameter in the direction orthogonal to the cleavage plane **(**$b_{KAP}$ = 1.331 nm**)**. This step is constituted by a double layer of acid phthalate ion held together by the potassium cation; it shows, as expected, the easy cleavage between the phenyl planes. Figure 2b shows the cleavage plane (010) of the KAP crystal, where the phenyl rows along $c_{axis}$ are clearly observed. The measured parameters along $a_{axis}$ (0.96 nm) and the angle (67°) between [101] and [10$\bar{1}$] are consistent with the given crystal parameters (space group $Pca2_1$, $a$ = 0.960 nm, $b$ = 1.331 nm, $c$ = 0.646 nm).[21,22] The superposed molecular model shows more clearly the molecular arrangement at the $(010)_{KAP}$ surface.

**Structure and Morphology of Symmetrical DCH Monomer Films: Epitaxial Growth of DCH Layers.** In the study of the oriented films, one important question to address is the growth mode of the epitaxial layers. To understand the first steps of monomer DCH

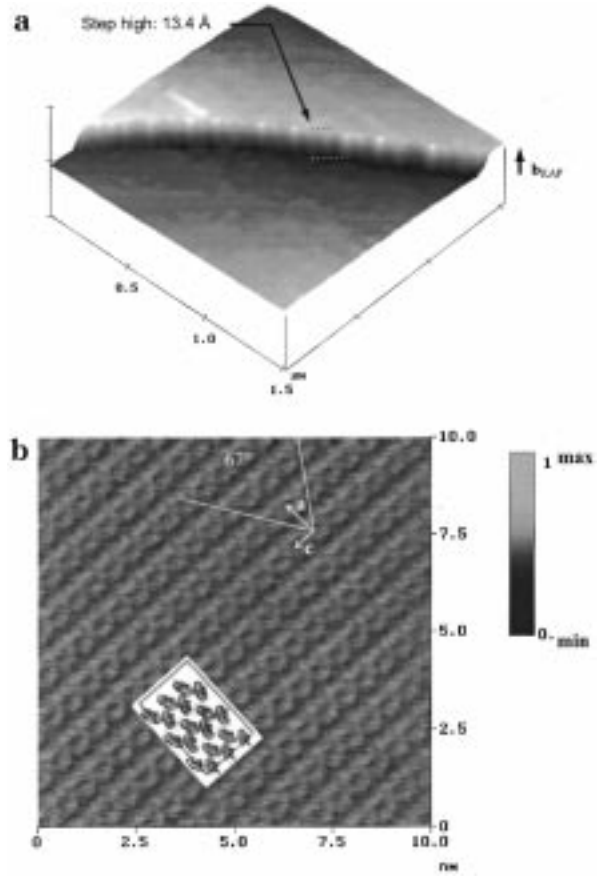


**Figure 2.** AFM pictures of the KAP surface: (a) single step on a KAP crystal face (010); (b) (010) face at the nanoscale. The molecular model simulation shows the crystal arrangement of the phenyl rings on the surface. Image scale 10 × 10 nm; $z_{max} = 2.0$ nm.

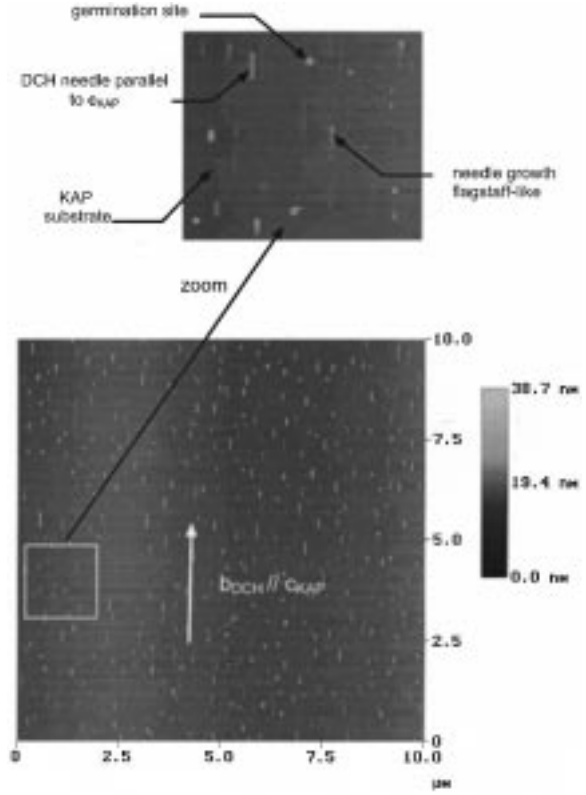


**Figure 3.** AFM picture of the DCH monomer film on KAP at low evaporation rate $E_r$. OMBE experimental conditions: $P_v$, $4.0 \times 10^{-8}$ mbar; $T_s = 25$ °C, $E_r \sim 0.02$ nm/min; equivalent thickness 0.2 nm. AFM surface picture: 10 × 10 $\mu m^2$; amplitude maximum $z_{max} = 60$ nm.

deposition on the KAP surface, the morphology is here investigated on thin films of small crystallites obtained at a low evaporation rate ($E_r \sim 0.02$ nm/min). The AFM picture **(**Figure 3**)** shows that the deposit on the crystal face occurs by random nucleation of small crystals. Zooming in on a part of the surface reveals several shapes for the crystals, which evolve from squares to bars and needles. Square crystals are the primitive nuclei, as demonstrated by our preliminary observations for lower amounts of deposited monomer (average equivalent film thickness ~0.1 nm) that yield only square and polygonal small nuclei. On a thicker film, barlike and needlelike crystals are well oriented along $c_{KAP}$. We thus infer that the square crystals should be considered as the nucleation sites of the long crystals of DCH, in which the *b* axis runs parallel to $c_{KAP}$. A careful inspection of the image and further control at high magnification of AFM (10 × 10 $nm^2$) reveals that the surface between DCH crystals is very flat, and the periodicities are characteristic of the (010) face of KAP, as seen in Figure 2b. It demonstrates that the observed KAP surface is free from DCH between the crystals. Consequently, it signifies also that the epitaxial growth proceeds by nucleation of crystallites separated by large bare areas without any diacetylene material.

The three basic modes of thin film growth by vapor deposition reported in the literature are (i) the layer by layer mode (Frank−van der Meeve mode), (ii) the three-dimensional crystallite growth (Volmer−Weber mode), and (iii) the mixed mode (Stranski−Krastanov mode). The last mode is defined as the growth of a monolayer followed by a 3D crystallite growth.[23,24] In this work we conclude that the epitaxial growth of DCH films on KAP proceeds by a Volmer−Weber mechanism. From the lack of monomer between crystals on the KAP it is clear also that during the first part of the evaporation, the DCH molecules are very labile, moving on the KAP surface toward the nucleation sites. The migration phenomenon is also well illustrated during the thermal polymerization. Parts a and b of Figure 4 show the AFM picture of a thin film before and after polymerization. A statistical analysis is performed on AFM pictures of Figure 4a,b. The mean crystal density per surface unity $\langle N_{cryst} \rangle = 11.6$ and 11.8 $\mu m^{-2}$ for parts a and b, respectively, and the fraction of the substrate crystal covered area (ratio of the total crystal area to the total surface in percent), $S_{cryst} = 11.9$ and 11.1% (for parts a and b), are not significantly different for the two pictures. Nevertheless, the mean ratio of the crystal length to crystal width $\langle L/l \rangle$ are respectively 10.5 and 3.6 before and after polymerization: this shows that during the heating-polymerization process, the surface diffusion of DA molecules modifies the crystal shape by reducing their length/width ratio. But as the overall crystal density and the covered surface remain unchanged, it points much more to a local diffusion within each crystal than its growth at the expense of others.

The evaporation rate effect is observed by comparison of Figures 4b and 5a for pDCH film obtained by evaporation at low rate $E_r \sim 0.36$ nm/min and high rate ~0.5 nm/s, respectively; with the substrate temperature held at 25 °C. The pDCH crystals are oriented in the same direction, parallel to $c_{KAP}$, but at low vaporization rates the needles are shorter and thinner than at high evaporation rates. Moreover, at high rates the crystal

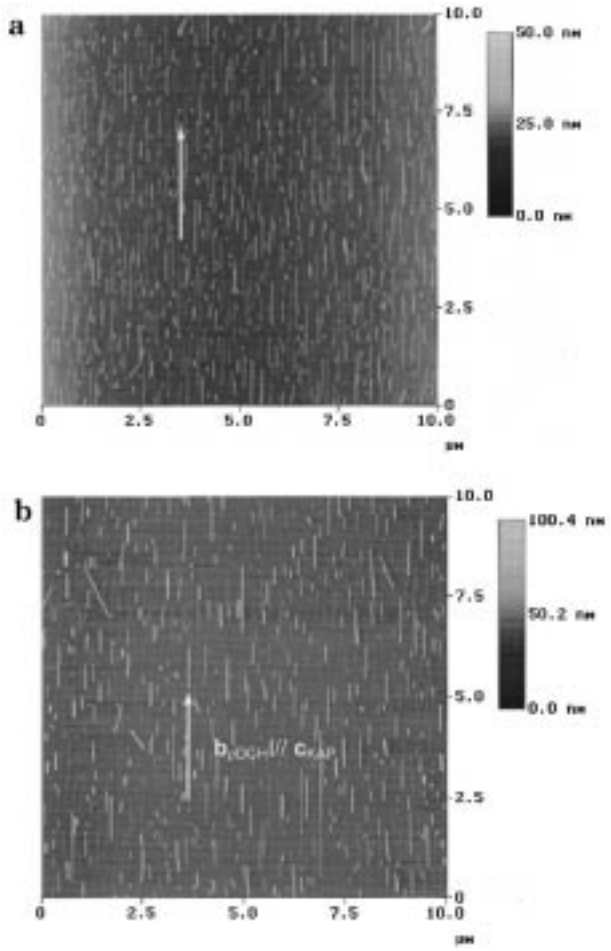


**Figure 4.** (a) AFM picture of the monomer DCH film grown at $T_s$ 25 °C. (b) AFM picture of the corresponding polymer pDCH film (polymerization condition, 150 °C, 24 h).

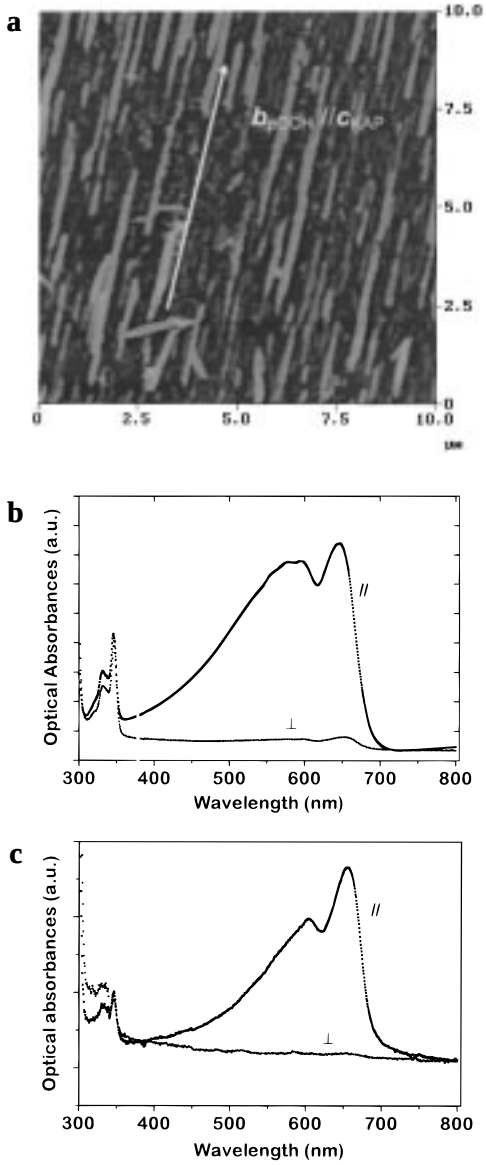


**Figure 5.** (a) AFM picture of the pDCH film evaporated at the high rate 0.5 nm/s, equivalent thickness 5.0 nm. In (b) and (c), the UV−vis absorption spectra respectively, $E_r \sim 0.5$ nm/s, equivalent thickness 77.5 nm, and $E_r \sim 0.36$ nm/min, equivalent thickness 47.0 nm. The polarized axes of the incident beam are respectively parallel and perpendicular to $c_{KAP}$.

shape is irregular and defects are numerous. Such morphological observations on oriented films can be correlated to their optical UV−vis absorption spectra measured with polarizers parallel and perpendicular to the polymer chain (Figure 5b,c). The shape of the absorption spectra and the lowest energy bands, corresponding to the exciton, are strongly different. At high rates, ∼0.5 nm/s, the absorption at maximum is at 646 nm (1.92 eV) and at low rates 0.36 nm/min, the absorption is red shifted at 656 nm (1.89 eV). These values of the low-energy exciton peaks agree with measurements on bulk single crystals by several authors.[25,26] The intensity at the exciton also changes as compared to the vibronic sidebands; the absorption ratio $A_x/A_{c=c} = 1.1$ in Figure 5b, while $A_x/A_{c=c} = 1.4$ in Figure 5c. At the same time the linear dichroic ratio at the exciton peak $A_{||}/A_{\perp}$ is respectively 15 and 25 for Figure 5b,c. Remember that we obtained a linear dichroic ratio as high as 61 for films evaporated at low rates on a substrate at 100 °C.[27] These optical results, which indicate a better ordering in slow rate conditions, corroborate the AFM morphological observations.

Figure 6a shows the AFM picture in vibrating mode of a single DCH needle and its cross-section perpendicular to the long axis. The $b_{DCH}$ axis is along the long axis of the crystal. The cross-section normal to $b_{DCH}$ reveals the contact face of the DCH crystal with the (010) plane of KAP. The cross-section shows a smooth shape without angle. This is due to convolution effects of the AFM tip with the solid, which depends on the shape, the angle of the tip, etc. However, within the experimental error, which is evaluated to 8−9°, the angles of the different faces are almost unchanged relative to the substrate face. Between the substrate surface taken as the reference and the faces AB, DE, and EF, the measured angles are respectively 52, 43, and 59° (see crystal section in Figure 6a). Considering the crystal monomer structure,[28] which is represented in Figure 6b, we propose the following indexations, $(\bar{2}03)_{DCH}$ for the contact plane with $(010)_{KAP}$, $(100)_{DCH}$ for AB, $(001)_{DCH}$ for DE, and $(104)_{DCH}$ for EF. The calculated values being 51.5, 42.5, and 60°, respectively. Taking into account the experimental error, the indexation of the $(\bar{2}03)_{DCH}$ contact plane is consistent with the previous indexation[13] $(\bar{1}02)_{DCH}$ of the natural growth face of DCH. The angle calculated from the crystalline structure between $(\bar{2}03)_{DCH}$ and $(\bar{1}02)_{DCH}$ is only 8.4°. Figure 6c shows the details of a polymer pDCH needle and its cross-section perpendicular to the long axis. The

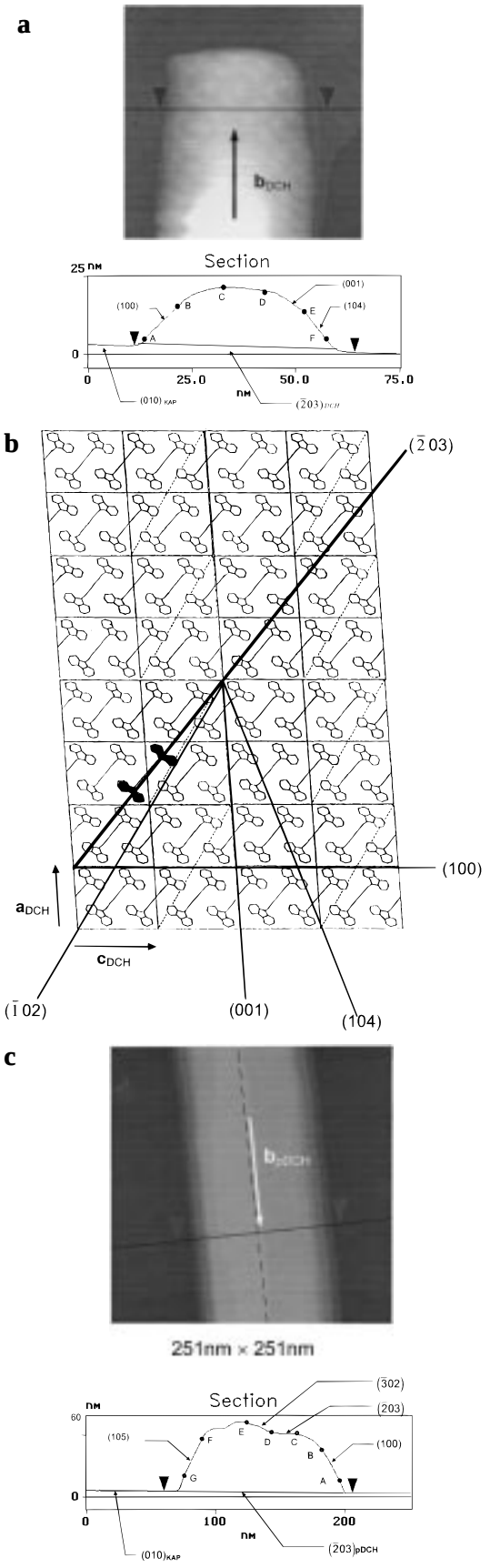


**Figure 6.** (a) AFM picture of a DCH needle and its cross-section along the indicated axis. (b) (010) DCH crystal model,[28] which shows the traces of some planes, parallel to the *b* axis. (c) Details of a pDCH needle and its cross-section perpendicular to the long axis.

$b_{pDCH}$ axis is the long axis of the crystal, and we index the different faces of the crystal as proposed in Figure 6c. This face indexation is based on a measured angle of 61° between $(100)_{pDCH}$ and $(\bar{2}03)_{pDCH}$, which should be 58.2° from the crystal model.

**Structure and Morphology of Asymmetrical Monomer Films.** The four asymmetrical DA with a single carbazolyl and different terminal urethane groups were used in order to check the molecular interaction of the carbazolyl DA derivatives with KAP. The monocarbazolyl derivatives were evaporated in the same experimental conditions as the DCH monomer on KAP.

After vacuum evaporation on KAP or on glass slides, none of the four monomers polymerizes directly after deposition at room temperature. As mentioned above, the monomers CNEU, CHPEU, and CHEU polymerize under UV light (254 nm) after thermal treatment respectively at 100, 120, and 100 °C. CNPEU after evaporation did not polymerize under any conditions. The absorption curves of polymers show two absorption groups at 320−345 and 550−650 nm. These absorption bands are characteristic, respectively, of the carbazolyl group and of the PDA conjugated chain. The more intense peak at lower energy, characteristic of the excitonic resonance was observed at 587, 595, and 622 nm, respectively, for pCNEU, pCHPEU, and pCHEU. Observed in polarized light by optical microscopy, the thin films of pCNEU and pCHPEU show a more or less intense dichroism along one or two specific directions.

For CHPEU, crystals of different shapes, needles, long flat crystals, and small nuclei, are observed on the AFM image. The majority of the crystals are randomly distributed on the surface, and a few of them are oriented along the privileged directions of KAP along *c* and at ±56° of *c*. CHEU and CNPEU did not show any privileged orientation.

For CNEU, the AFM images are given in Figure 7a−c for different steps respectively, after evaporation at room temperature, after thermal treatment, and after photopolymerization. Figure 7a shows smooth crystals in a mosaic arrangement not well oriented. After a thermal treatment (100 °C, 1 min) the crystal shape and size change drastically (Figure 7b), and long needle crystals grow along $c_{KAP}$ and also at 57° or 122° from $c_{KAP}$. All the crystals are distributed along these three main directions. The polymer crystals are longer than the monomer crystals for the same film (Figure 7c), and the orientations are easily observed due to the elongated shape of the crystals. At the same time, some defects can be observed at the surface, such as crystal curvatures or growth along other specific directions. These observations indicate that different specific molecular interactions can occur during the crystal growth. The long axis of pCNEU crystals is along the *three directions*, $c_{KAP}$, $[101]_{KAP}$, and $[10\bar{1}]_{KAP}$, the two having a typical angle of 67° between them that we quoted in Figure 2b.

By changing the evaporation rate or the temperature of the KAP substrate for DCH, we have been able to modify the morphology of the film grown by epitaxy. Analogous results are observed by AFM on an oriented film of pCNEU (Figure 7d) grown by evaporation at slow rates on the KAP at 100 °C. The morphological observations are corroborated by bright field TEM observations (Figure 8a). The electron diffraction pattern (Figure 8b) shows the organization in different layers; the repetitive distance is 0.48 nm, which is character-

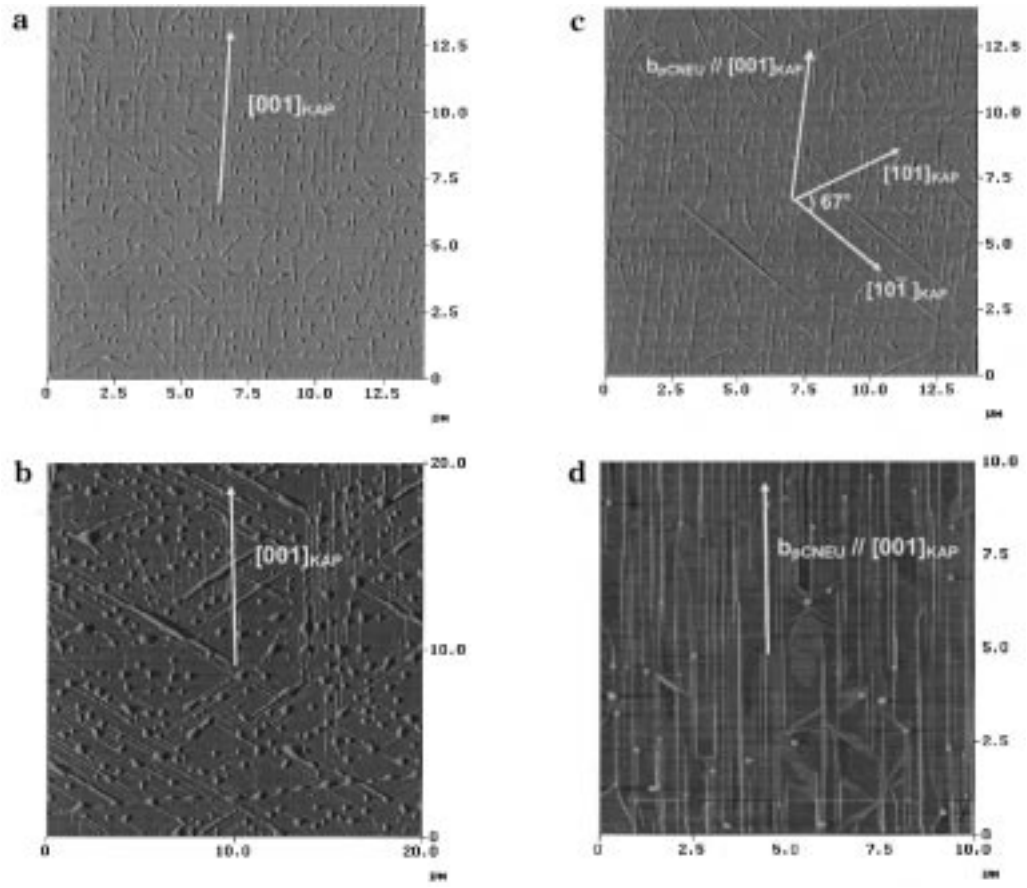


**Figure 7.** AFM pictures of CNEU monomer and polymer on KAP. (a) AFM structure of the monomer just after the evaporation, equivalent thickness 1.0 nm, $E_r = 0.05$ nm/min, deposited at room temperature. (b) Same film after a thermal treatment at 100 °C, 1 min. (c) Polymerized pCNEU film after UV irradiation. (d) the AFM picture of a thicker film of pCNEU deposited on KAP at 100 °C. Equivalent thickness = 7.2 nm, $E_r = 0.125$ nm/min.

istic of the repetitive distance along the chain axis for polydiacetylenes[29] (0.491 nm for PTS, 0.488 nm for BCMU, 0.491 nm for DCH). The chain axis runs along the long axis of the needles. Though the crystal structure of CNEU has not been determined to be consistent with the denomination for DCH, we call *b* the chain axis. The main orientation of crystals is again parallel to the $c_{KAP}$ axis, i.e., $b_{CNEU}$ and $b_{pCNEU}$ parallel $c_{KAP}$. Only a few crystals are still oriented along the two other directions, $[101]_{KAP}$ or $[10\bar{1}]_{KAP}$. The two orientations along the ⟨101⟩ directions are revealed by bright field images but do not appear on the diffraction pattern, demonstrating that $[101]_{KAP}$ or $[10\bar{1}]_{KAP}$ can be considered as secondary directions for the epitaxial growth of the CNEU.

This is confirmed at the macroscopic level by UV−vis absorption spectra in Figure 8c, which were measured with the polarizers parallel and perpendicular to $b_{pCNEU}$. A high absorption ratio (16) is observed at 587 nm. This strong dichroism shows that the secondary orientations can be well minimized during the epitaxial growth of CNEU. This is also in agreement with the nonlinear optical dichroism already observed for the CNEU epitaxied films. It confirms also the interest of the epitaxy, compared to the rubbing technique. As we have shown previously, the optical dichroism was higher for the pCNEU film oriented by epitaxy than for the p4BCMU oriented by rubbing (see table and Figures 4 and 5 in ref 14).

From all these observations we can assume that the molecular interaction with the crystal substrate is in part due to the carbazolyl interaction with the phenyl at the crystal surface. From the epitaxial relationships in DCH/KAP systems,[13] we concluded in a first paper that the monomer orientation was driven by the molecular insertion of the carbazolyl groups in privileged sites of the KAP surface. In this work we propose a model for the molecular insertion of the CNEU monomer as compared with the DCH monomer in parts b and a of Figure 9, respectively. It means that the specific molecular interaction between the carbazolyl group and the phthalate surface can be *extended* to other molecules bearing a single carbazolyl site. The other substituent of DA is also able to interact with the KAP surface. Therefore, the molecular orientation is due to several effects, for the predominant orientation a $\pi-\pi$ interaction based on the insertion of the carbazolyl group at the $(010)_{KAP}$ face and a geometrical interaction leading to a preferential orientation of the polymer chain along the $c_{KAP}$ axis. Then, two secondary orientations of the polymer chain along the [101] and $[10\bar{1}]$ of KAP are possible, quite analogous to that observed for polyethylene on KAP.[30]

By using the epitaxial relationships observed for pCNEU, a possible molecular model is given in Figure 9c. It shows that, if the position of the DA monomer is given by the carbazolyl group, the chain orientations are controlled by the urethane side groups along the phthalate rows. When the urethane group runs along $[101]_{KAP}$ or $[10\bar{1}]_{KAP}$, the resulting growth direction of the polymer chain, $b_{pCNEU}$, is parallel to $c_{KAP}$. The urethane group can also be oriented along $c_{KAP}$, and the

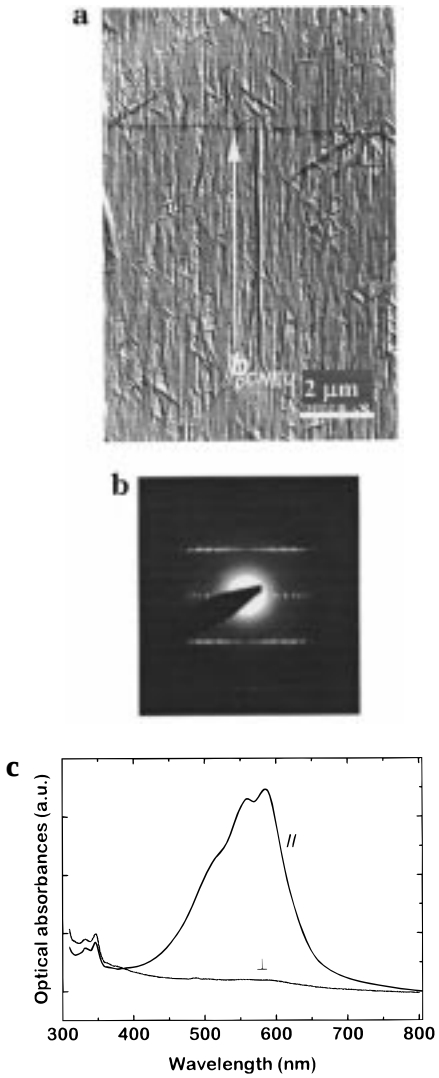


**Figure 8.** (a) TEM bright field image of the pCNEU on KAP, equivalent thickness = 23 nm. (b) Electron diffraction pattern representative of the main orientation. (c) UV−vis spectra of the oriented film. The polarized axis of the incident beam is respectively parallel and perpendicular to $c_{KAP}$.

resulting $b_{pCNEU}$ growth directions are parallel to $[101]_{KAP}$ or $[10\bar{1}]_{KAP}$ by symmetry. It signifies too that the single carbazolyl group in a diacetylene monomer induces a lower order than the twin carbazolyl groups of the DCH monomer. Related to the thin film morphologies, the strong dichroism of well oriented PDA is observed on pCNEU as in pDCH. The improvements in orientational order are strongly dependent on evaporation conditions, i.e., slow evaporation rate and moderate heated substrate (50−100 °C).

## Conclusion

We investigated the oriented overgrowth of a series of carbazolyl derivatives of diacetylene monomers by *epitaxy* on a single-crystal surface of potassium acid phthalate (KAP). By changing the chemical architecture of the deposited molecule, we are able to modify the molecular interactions between the deposited molecule and the crystal surface. We demonstrated, for the *monosubstituted carbazolyl derivative pCNEU*, that the molecular interactions leading to epitaxy are of several types. First, a geometrical interaction favored by $\pi-\pi$ interactions (carbazolyl to phenyl), based on the insertion of the single carbazolyl group on the KAP (010) face, induces the *position* of the DA. Second, a geometrical interaction (DA side chain to KAP surface rows) leads to three *preferential orientations* of the polymer chain, *a main direction* along the $c_{KAP}$ axis and two *secondary directions* along the [101] and $[10\bar{1}]$ of KAP. Related to the thin film morphologies, static optical spectroscopy demonstrates that improvements in orientational order are observed on both pCNEU and pDCH at slow evaporation rates and on heated crystal substrate in the temperature range 50−100 °C.

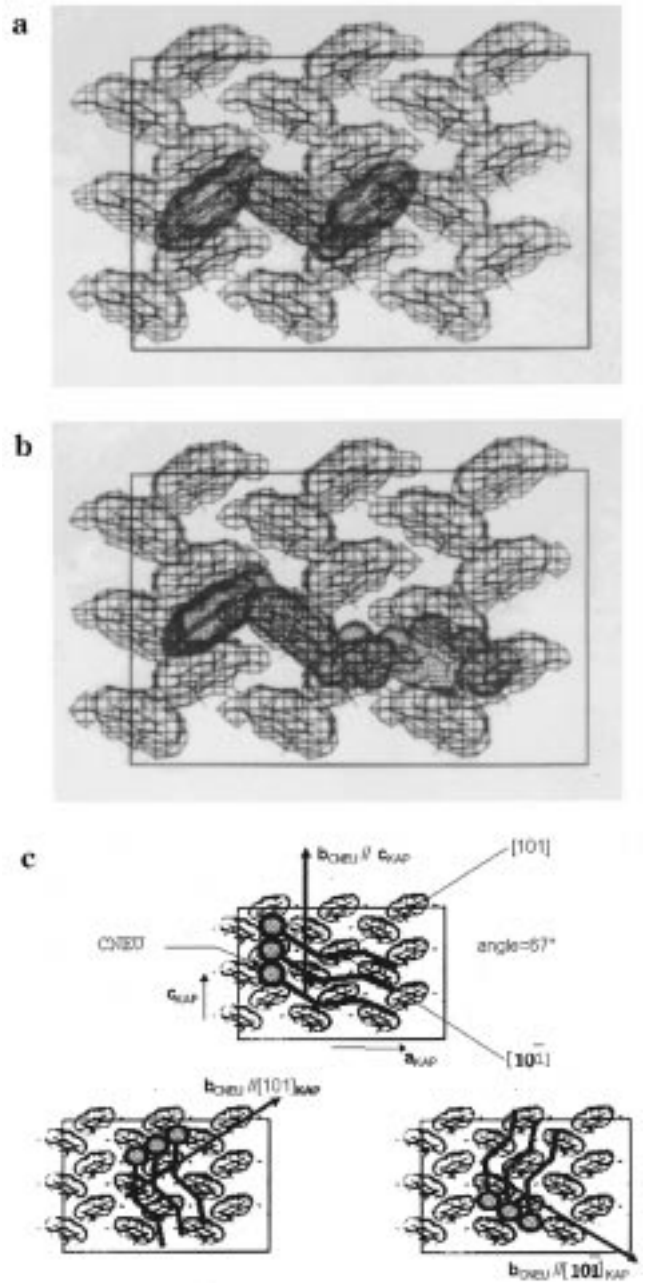


**Figure 9.** Molecular models of (a) DCH and (b) CNEU, respectively, on the KAP surface. For CNEU the three possible orientations of the carbazolyl and urethane groups on the KAP surface are presented in (c).

**Acknowledgment.** We wish to acknowledge the CNRS and the MRT (grant no. 91.S.0424). We would like also to thank Mr. M. Keyser and the Analytical Services Group of the Institut Charles Sadron in Strasbourg for the elemental analyses. We would like also to

thank Mr. M. Romeo for his helpful contribution to the statistical analysis of the AFM pictures.

## References and Notes

(1) Samant, M. G.; Stöhr, J.; Brown, H. R.; Russell, T. P.; Sands, J. M.; Kumar, S. K. *Macromolecules* **1996,** *29*, 8334.
(2) Wittmann, J. C.; Smith, P. *Nature* **1991**, *352*, 414.
(3) Thakur, M.; Meyler, S. *Macromolecules* **1985,** *18*, 2341.
(4) Hara, M.; Sasabe, H.; Yamada, A.; Garito, A. *Jpn. J. Appl. Phys.* **1989**, *28*, L306.
(5) Dann, A.; Hoshi, H.; Maruyama, Y. *J. Appl. Phys.* **1990**, *67*, 1371.
(6) Ueda, Y.; Kuriyama, T.; Hattori, Y.; Uenishi, N.; Uemiya, T.; Ashida, M. *Thin Solid Films* **1993**, *227*, 181.
(7) Forrest, S.; Burrows, P. E.; Haskal, E.; Zhang, Y. *Mater. Res. Soc. Symp. Proc.* **1994**, *328*, 37.
(8) Kanetake, T.; Tomioka, Y.; Imazeki, S.; Taniguchi, Y. *J. Appl. Phys.* **1992**, *72*, 938.
(9) Le Moigne, J.; Oswald, L.; Kajzar, F.; Thierry, A. *Nonlinear Opt.* **1995**, *9*, 187.
(10) Pham, T. A.; Daunois, A.; Merle, J. C.; Le Moigne, J.; Bigot, J. Y. *Phys. Rev. Lett.* **1995**, *74*, 904. Bigot, J. Y.; Pham, T. A.; Daunois, A. *Photonics Sci. News* **1996**, *2*, 6.
(11) Sauteret, C.; Hermann, J. P.; Frey, R.; Pradère, F.; Ducuing, J.; Baughman, R.; Chance, R. R. *Phys. Rev. Lett.* **1976**, *36*, 956.
(12) Enkelmann, V.; Leyrer, R. J.; Schleier, G.; Wegner, G. *J. Mater. Sci.* **1980**, *15*, 168.
(13) Le Moigne, J.; Kajzar, F.; Thierry, A. *Macromolecules* **1991**, *24*, 2622.
(14) Kajzar, F.; Lorin, A.; Le Moigne, J.; Szpunar, J. *Acta Phys. Polon.* **1995**, *A87*, 713.
(15) Bloor, D. In *The Polymerization of Disubstituted Diacetylene Crystals*; *Developments in Crystalline Polymers;* Basset, D. C., Ed.; Applied Science Publishers: London, 1982; Chapter 4, p 157.
(16) Yee, K. C. U.S. Patent 4,125,534, 1978.
(17) Krönke, C. *Ber. Bunsen-Ges. Phys. Chem.* **1987**, *91*, 982.
(18) Le Moigne, J.; Thierry, A.; Chollet, P. A.; Kajzar, F.; Messier, J. *J. Chem. Phys.* **1988**, *88*, 6647.
(19) Yee, K. C.; Chance, R. R. *J. Polym. Sci., Polym. Phys. Ed.* **1978**, *16*, 431.
(20) Binnig, G.; Quate, C. F.; Gerber, C. *Phys. Rev. Lett.* **1986**, *56*, 930.
(21) Okaya, Y. *Acta Crystallogr.* **1965**, *19*, 879.
(22) The structure definition used here corresponds to the structure data of Okaya[21] corrected by R. A. Smith (*Acta Crystallogr.* **1975**, *B31*, 1773) and presented under the standard setting, $Pca2_1$.
(23) Kern, R. *Bull. Minéral.* **1978**, *101*, 202.
(24) Venables, J. A. *Surf. Sci.* **1994**, *798*, 299.
(25) Tomioka, Y.; Imazeki, S. *J. Phys. Chem.* **1991**, *95*, 7007.
(26) Morrow, M. E.; White, K. M.; Eckhardt, C. J.; Sandman, D. J. *Chem. Phys. Lett.* **1987**, *140*, 263.
(27) Da Costa, V.; Le Moigne, J.; Pham, T. A.; Bigot, J. Y. *Synth. Met.* **1996**, *151*, 81.
(28) Enkelmann, V.; Schleier, G.; Wegner, G.; Eichele, H.; Schwoerer, M. *Chem. Phys. Lett.* **1977**, *52*, 314.
(29) Enkelman, V. In *Advances Polymer Science*; *ACS series 63*; Cantow, Ed.; Springer-Verlag: Berlin, 1984; pp 92−133.
(30) Wittmann, J. C.; Lotz, B. *J. Polym. Sci., Polym. Phys. Ed.* **1981**, *19*, 1837.

MA971177P